参赛队员姓名：黄丹忱

中学：北京一零一中学

省份：北京

国家/地区：中国

指导教师姓名：孙晓明

指导教师单位：北京化工大学

论文题目：The Synthesis of Nb-doped NiFe-LDH Nanoarray and its Electrocatalytic Performance on the Anode of Water Electrolysis

论文题目：The Synthesis of Nb-doped NiFe-LDH Nanoarray and its Electrocatalytic Performance on the Anode of Water Electrolysis

作者：黄丹忱

论文摘要：

Oxygen evolution reaction (OER) is a half-cell reaction of water electrolysis which produces hydrogen that is a key solution to energy problems. However, the kinetic performance of OER still has much room for improvement for it involves the transfer of four electrons. In this work, we focused on the doping method of the NiFe layered double hydroxide (NiFe-LDH) that serve as OER catalysts. We also investigated the improvement of the catalyst transfer media. The Nb-doped NiFe-LDH not only uses cheap and abundant non-noble metals but is also characterized by excellent OER performances, high mass transfer efficiency, and improved OER kinetics. It provides inspiration for catalyst design in this field.

关键词：Layered double hydroxide, nanoarray, water splitting, oxygen evolution reaction, doping

目录：

1. Introduction.....4
2. Methodology.....6
    2.1 Materials.....6
    2.2 Synthesis of NiFe-LDH.....6
    2.3 Synthesis of Nb-doped NiFe-LDH.....6
    2.4 Synthesis of Nb-doped NiFe powder electrode.....6
    2.5 Characterization.....6
    2.6 Electrochemical measurement.....7
3. Results and Discussion.....8
4. Conclusions.....13
5. References.....15
6. Acknowledgement.....16

论文正文：

1. Introduction

Many countries in the world have recognized the importance of reducing carbon dioxide emissions, and with the depletion of traditional energy sources such as petroleum, some political goals have been articulated. For instance, China released an action plan to reach the carbon dioxide emissions peak before 2030 and achieve carbon neutrality before 2060[1]. To accomplish these goals, it is urgent to develop green energy other than traditional fossil energy. Hydrogen is the most promising non-carbon-based energy source that could meet national carbon reduction targets, due to its high energy density. The industrial progression of hydrogen energy relies heavily on the production of hydrogen, which is the upstream of the industrial chain for hydrogen energy. The speed and quality of hydrogen production and the advancement of this technique directly determine the maturity of the whole hydrogen energy industrial chain. Thus, there is an urgency to improve the hydrogen production technology.

Three methods are commonly used to produce hydrogen[2]. One method generates hydrogen from fossil fuel and the hydrogen thus produced is called "grey hydrogen". Although hydrogen itself only produces water when it burns and does not pollute the environment with carbon emissions, the manufacturing process of the grey hydrogen, though cheap, emits large amounts of carbon dioxide and heavily pollutes the environment. The second method produces "blue hydrogen" from natural gas. The method also produces carbon dioxide, but the carbon dioxide is captured and stored. The third method generates "green hydrogen" by water electrolysis, and it is powered by clean energy sources. Thus, this operation is considered perfectly environmentally friendly.

The water electrolysis method is commonly acknowledged as the most advantageous and the cleanest way to generate hydrogen. It can benefit the whole energy industrial chain in diverse ways. Hydrogen is not only an excellent fuel but can also be used to promote other types of procedures to yield renewable energies, such as solar energy, wind energy, and geothermal energy. These kinds of renewable energy are being rapidly developed. They are used in a wide range. For instance, China's total installed capacity of wind power has reached 31 billion watts[3]. However, renewable energies face the

problem of energy curtailment. Water electrolysis can help solve this problem by storing the energy produced at the production peak by wind turbines, solar panels, and other production measures of different renewable energy sources and turning their electric energy into chemical energy. Then, at the production bottom, hydrogen can be used to convert the stored chemical energy to electric energy by reverse reaction. However, the high energy consumption of water electrolysis and the low energy conversion efficiency create a bottleneck in hydrogen production. Therefore, it is necessary to develop high-performance electrocatalysts for water electrolysis.

There are two half-cell reactions in the process of water electrolysis. The first one occurs on the cathode and yields hydrogen (hydrogen evolution reaction, HER) while the second one occurs on the anode and yields oxygen (oxygen evolution reaction, OER). Since the HER involves the transfer of two electrons while the OER involves the transfer of four electrons, the half-cell reaction that occurs on the anode has a poor kinetic performance while consuming large amounts of energy[4]. In addition, the potential required for the OER is always higher than the theoretical potential (1.23 V vs reversible hydrogen electrode, or RHE), with the exceeding amount called overpotential. In recent studies, noble metals have been a good option to decrease the overpotential, and IrO_2 and RuO_2 are the most commonly used OER electrocatalysts[5]. However, noble metals are both scarce and expensive, which will probably create a bottleneck in the industrial chain if relatively cheaper catalysts are not developed. Among all the elements, transition metals are characterized by both abundance and low cost. These qualities have made them appealing substances for catalysts.

The NiFe layered double hydroxide (NiFe-LDH) has proven to have excellent OER performance in alkaline environments, among all kinds of non-noble metal based catalysts. However, its performance and stability need to be further enhanced for use in real work conditions. OER performance can usually be improved in two different ways. One way is to improve its intrinsic activity. The approaches employed for this purpose include element doping, constructing defects, and surface engineering. Among them, doping is regarded as a relatively efficient and simple method. Another way to improve the performance is accelerating the mass transfer. Compared with powder electrodes, which tend to adhere to product bubbles and therefore experience a barrier effect, the

self-supporting nanoarray electrodes could achieve a significant improvement in mass transfer and thus in the rate of current increase[6].

In this work, we adopted the Niobium (Nb) doping method to enhance the intrinsic activity of the NiFe-LDH. We constructed the Nb-doped NiFe-LDH as a self-supporting nanoarray that is grown on the Nickel foam substrate (Nb/NiFe-LDH). This strategy greatly improved the intrinsic activity of the NiFe-LDH and accelerated the gas-liquid mass transfer efficiency. The Nb/NiFe-LDH required only 200 mV overpotential to aquire a current density of 10 mA cm^{-2}, and could work stably for hundreds of hours at ampere-level current density.

2. Methodology

2.1 Materials:

Various chemicals were used in this study. $Fe(NO_3)_2 \cdot 9H_2O$ (99.99%), $NbCl_5$ (99.9%) and Nickel(II) Acetyl Acetonate ($Ni(acac)_2$, 99%) were purchased from Aladdin Industrial Co. Urea (99%) and ethanol (99.9%) were purchased from Beijing Chemical Reagents Co. Carbon fiber paper was purchased from Toray Industries, Inc. Deionized water with a resistivity ≥ 18 MΩ was used to prepare all aqueous solutions. All the reagents were of analytical grade and were used directly without further purification.

2.2 Synthesis of NiFe-LDH:

Firstly, 1 mmol $Ni(acac)_2$, 1 mmol $Fe(NO_3)_2 \cdot 9H_2O$, and 0.3 g urea were dissolved in 30 mL deionized water. Then this solution and a piece of 2*4 cm^2 cleaned Ni foam was transferred into the Teflon-lined stainless autoclave and maintained at 120°C for 12 h to obtain the NiFe-LDH nanoarray.

2.3 Synthesis of Nb/NiFe-LDH:

Firstly, 1 mmol $Ni(acac)_2$, 0.8 mmol $Fe(NO_3)_2 \cdot 9H_2O$, 0.2 mmol $NbCl_5$ and 0.3 g urea were dissolved in 30 mL deionized water. Then this solution and a piece of 2*4 cm^2 cleaned Ni foam was transferred into the Teflon-lined stainless autoclave and maintained at 120°C for 12 h to obtain the Nb/NiFe-LDH nanoarray.

2.4 Characterization:

Scanning Electron Microscope: Zeiss SUPRA55 scanning electron microscope was used in this work, which was operated at 10 kV. The scanning electron microscope (SEM)

was used to characterize the morphology and size of the powder and nanoarray samples. Moreover, the SEM-EDS mapping, which is an elemental analysis technique, helped us further identify the materials and provided us with a view of the elemental compositions of the materials.

X-ray diffraction: In this test, Bruker D8 Advance with Cu Kα radiation which has λ=1.5418Å was used to produce X-ray diffraction (XRD) graphs, which showed the microstructure, the structure of the crystal, and the size of the crystal grains. The diffraction patterns and diffraction angles of the graphs together helped to determine the crystal phases of the samples. They also indicated the structure of the samples by helping to deduce the spacing of the crystal planes.

X-ray photoelectron spectroscopy: X-ray photoelectron spectroscopy (XPS) contributed to determining the composition and distribution of our samples. It characterized the composition on the surface of the material, the types of elements, and the valence numbers.

Bubble performance test: The contact angle was derived by using the captive bubble method and Dataphysics DCAT21. The bubble performance was characterized by the contact angles. The test helps to show the qualities of the catalytic media.

2.5 Electrochemical measurement:

The electrochemical measurements for OER were performed in a standard three-electrode system at room temperature on an electrochemical workstation (CHI 660D, Chenhua, Shanghai), where the NiFe-LDH, Nb/NiFe-LDH, Nb/NiFe-LDH (powder) served as the working electrodes, while Pt foil electrodes and SCE electrodes served as counter electrodes and reference electrodes, respectively, and 1 M KOH was used as the electrolyte. The LSV and CV tests at a scan rate of 2 mV/s were performed after 40 cycles of CV. The final potentials were converted with respect to the reversible hydrogen electrode (RHE) based Nernst equation: E (RHE, iR corrected) = E (SCE) + 0.244 V + 0.059 pH – iR, where *i* is the measured current density and *R* is the solution resistance determined by EIS. The Tafel plots were derived from the polarization curves. The stability tests were performed in a two-electrode system by chronopotentiometry measurements at 0.01 A cm^{-2}, 0.1 A cm^{-2}, 0.5 A cm^{-2} and 1 A cm^{-2}.

3. Results and Discussion

The NiFe-LDH and Nb/NiFe-LDH electrocatalysts were prepared on the Nickel foam (NF) via a one-step hydrothermal approach (Figure 1A). In this process, $Ni(acac)_2$ was used to provide $acac^{2-}$, thus to prevent the possible hydrolysis of Nb^{5+}. Figure 1B and Figure 1C show the SEM images of NiFe-LDH and Nb/NiFe-LDH, respectively. They display the uniformly grown LDH nanoarray on the NF and the process of Nb doping without affecting the initial morphology of NiFe-LDH, respectively. As can be seen from the SEM image in Figure 1C, the as-synthesized Nb/NiFe-LDH shows an ultrathin two-dimensional (2D) structure. This unique 2D structure can help to expose more active sites of the Nb/NiFe-LDH, and is expected to provide hydrophilic and hydrophobic properties for the nanoarray. The energy dispersive X-ray spectroscopy mapping (EDS-Mapping) of SEM in Figure 1D proves that Ni, Fe, and Nb are uniformly distributed, and there is no agglomeration formed by Nb_2O_5 powder particles stuck together. This result shows the successful homogeneous doping of Nb^{5+} and demonstrates that Nb^{5+} can be stabilized by the complexation of $acac^{2-}$ to prevent its hydrolysis.

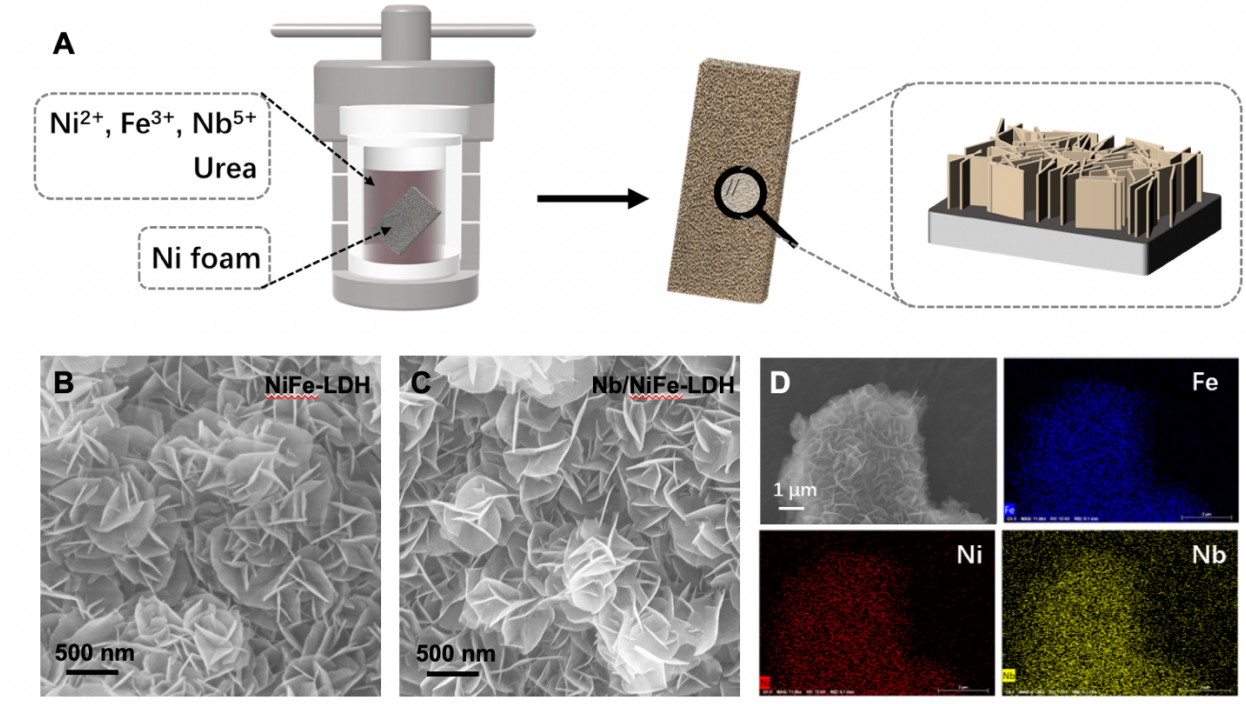

Figure 1. (A) Schematic route for the synthesis of CoFePBA/Co_2P electrode. (B) SEM image of NiFe-LDH. (C) SEM image of Nb/NiFe-LDH. (D) SEM image and corresponding EDS elemental mapping for Ni, Fe and Nb of Nb/NiFe-LDH.

Then the composition of the as-synthesized catalyst was further analyzed, and the structures of the as-synthesized NiFe-LDH and Nb/NiFe-LDH were confirmed by XRD (Figure 2A), in which the diffraction peaks corresponding to the lattice planes of the NiFe-LDH (NiFe-LDH--JCPDS#40-0215) are clearly visible. This proves that Nb doping will not lead to the phase separation or crystal transformation of the material. Moreover, from the diffraction fringes of the (006) plane that is located at about 23 °, it can be observed that, compared with the NiFe-LDH, the Nb/NiFe-LDH has a deflection toward smaller angles. This phenomenon means that Nb^{5+} ions with relatively big radii were doped into the NiFe-LDH. By using the Bragg Law ($2d \sin\theta = n\lambda$), which states the relationship between the variables concerning diffraction, the spacing between crystal planes can be determined. It was deduced that the crystal plane spacing for the NiFe-LDH is about 0.398 nm. However, after Nb was doped, the (006) plane increased to about 0.408 nm. This further proves the success of the doping of Nb.

XPS survey was performed to obtain more evidence of Nb doping. As shown in Figure 2B, the absence of signals for Nb 4s in the spectra of the NiFe-LDH further confirms the successful Nb doping. Then the atomic ratio in Nb/NiFe-LDH was detected by EDS. It can be seen from Figure 2C that Ni, Fe and Nb accounted for 53.21%, 38.53% and 8.26% of the LDH, respectively. The experimental results are close to the theoretical values.

The high-resolution XPS spectrum of Ni 2p (Figure 2D) shows a pair of peaks located at 855 and 875 eV, corresponding to Ni^{2+} $2p_{3/2}$ and $2p_{1/2}$ spin orbitals, respectively. The other peaks are assigned to satellite peaks (sat.). In Figure 2E, the peaks centered at 713 and 725 eV are ascribed to the $2p_{3/2}$ and $2p_{1/2}$ of Fe^{2+}. Note that the oxidation state of Ni does not change obviously after Nb doping, but the peak of Fe^{2+} $2p_{3/2}$ shifted 1.68 eV toward high binding energy. This phenomenon indicates that the doped Nb attracts the electrons of Fe and decreases the electron cloud density around Fe, thus maintaining a relatively high oxidation state. Moreover, three peaks corresponding to O defect, M-OH, and M-O, respectively, can be observed in Figure 2F. After Nb doping, the proportion of

O defect increased noticeably. This may be caused by the change in the coordination environment due to the doping of high valence Nb^{5+}. It has been reported that the generate of O defect benefits the OER performance by exposing more active sites[4].

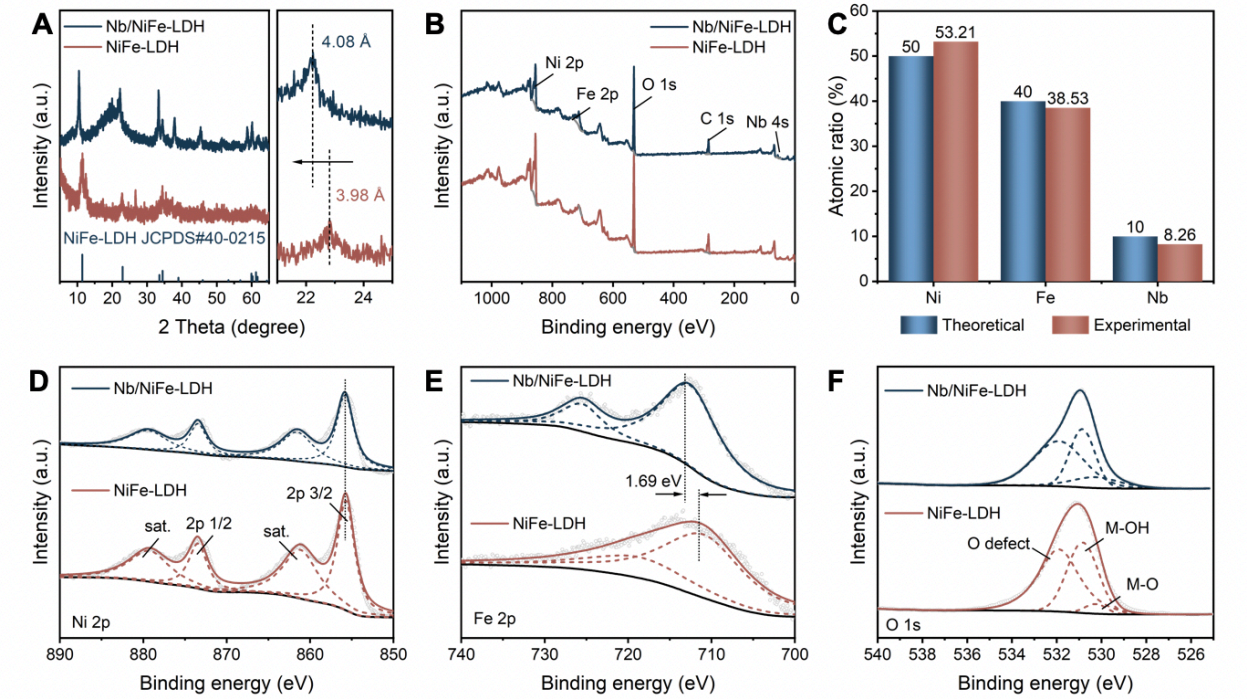

Figure 2. (A) XRD patterns of Nb/NiFe-LDH and NiFe-LDH. (B) XPS survey of Nb/NiFe-LDH and NiFe-LDH. (C) Atomic ratios of Ni, Fe and Nb in Nb/NiFe-LDH, detected by SEM-EDS. High-resolution XPS spectra of (D) Ni 2p, (E) Fe 2p and (F) O 1s of Nb/NiFe-LDH and NiFe-LDH.

The OER performance of the Nb/NiFe-LDH and NiFe-LDH electrodes were examined in an alkaline electrolyte (1 M KOH). As shown in Figure 3A, Nb/NiFe-LDH exhibited prominent catalytic activity toward OER requiring only an overpotential of 200 mV, which is lower than that in the NiFe-LDH (286 mV), to reach a current density of 10 mA cm^{-2}. Note that the Ni foam did not show any activity toward OER within the investigated potential range. Moreover, the Nb/NiFe-LDH possessed a smaller Tafel slope of 17.3 mV dec^{-1} (Figure 3B) compared with the NiFe-LDH (32.1 mV dec^{-1}) and Ni foam (47.5 mV dec^{-1}), demonstrating the favorable OER catalytic kinetics for the Nb/NiFe-LDH.

The redox peaks of these sample are shown in Figure 3C, and a much higher oxidation peak and lower reduction peak of Ni^{2+}/Ni^{3+} can be observed. This demonstrates that the Ni^{2+} in NiFe-LDH is much easier to oxidize after Ni doping. Furthermore, a pair of Ni^{3+}/Ni^{4+}

redox peaks appear in the curve of the Nb/NiFe-LDH at about 1.43 V vs RHE, and the Ni^{4+} has been reported to be an OER active site in the NiFe-LDH[4]. This indicates that the doping of Nb can make it easier to oxidize Ni in the OER process, thus producing a large number of active sites at a lower potential. This can explain why the Nb/NiFe-LDH exhibits better OER performance and more favorable OER kinetics than the NiFe-LDH.

The stability of the Nb/NiFe-LDH is shown in Fig 3D. The stability of the Nb/NiFe-LDH was tested in a two-electrode system. Commercial Ni foam was selected as the cathode. The test was carried out in the range of 0.01 A cm^{-2} to 1 A cm^{-2}. The as-prepared electrode was tested at each current density for 100 hours. It can be noted that only negligible catalyst performance attenuation can be observed during the whole test, verifying the excellent long-term stability of the Nb/NiFe-LDH. Besides, the Nb/NiFe-LDH can maintain its exceptional capability even when working under large currencies for a long time.

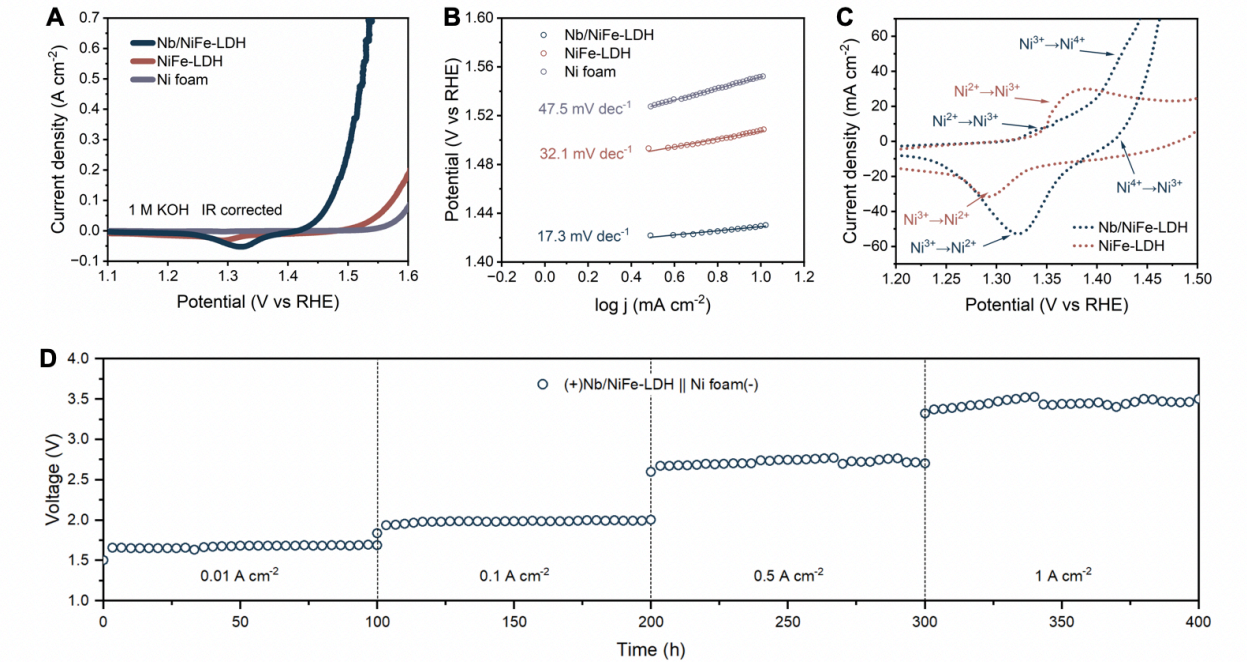

Figure 3. (A) Polarization curves of Nb/NiFe-LDH, NiFe-LDH and Ni foam. (B) Tafel plots of Nb/NiFe-LDH, NiFe-LDH and Ni foam. (C) Redox peak of Nb/NiFe-LDH, NiFe-LDH and Ni foam, detected by CV. (D) Stability test of Nb/NiFe-LDH at current density of 0.01 A cm^{-2}, 0.1 A cm^{-2}, 0.5 A cm^{-2} and 1 A cm^{-2}.

Beyond the intrinsic activity, the mass transfer ability is also important, which is usually related to the current increases rate. The OER performance of the Nb/NiFe-LDH in

different states were tested. As can be seen in Figure 4A, the Nb/NiFe-LDH (nanoarrays) and the Nb/NiFe-LDH (powder) demonstrate similar onset potential. However, the nanoarrays exhibit much better performance at high current densities. We also analyzed the current increase rate by the Tafel slope (Figure 4B). At the beginning, the Nb/NiFe-LDH possessed similar Tafel slopes of about 20 mV dec^{-1}, which indicates that they have the same intrinsic activity. However, at high current densities, the Nb/NiFe-LDH (nanoarrays) needed only 69.4 mV to increase the current density by ten fold, while the Nb/NiFe-LDH (powder) required 145.4 mV. This shows that growing electrocatalysts into nanoarrays is conducive to a more rapid growth of current density.

Then we tested the mass transfer performance of the Nb/NiFe-LDH (nanoarrays). As shown in Figure 4C and Figure 4D, the as-prepared electrode shows excellent wettability, requiring only 300 ms to be wetted and showing no solid-liquid contact angle. This demonstrates the super-hydrophilicity of the nanoarray sample. The hydrophilic quality of the sample is conducive to invoking all the active sites in the nanoarray sample. Moreover, the Nb/NiFe-LDH can help to reduce the stacking effect on the catalyst and enhance the mass transfer from the reactant to the active sites. The contact angle with the bubble in the electrolyte is CA_{bubble} = 157°. This shows that our nanoarray material possesses the quality of superaerophobicity that can decrease the gas bubble adhesion and increase the bubble contact angle, thus releasing the gas bubbles faster and improving the sample's electrocatalytic performance in terms of the current increase rate and stability[7]. This quality of the sample helps to quickly transmit the reactant in the electrolyte to the active sites.

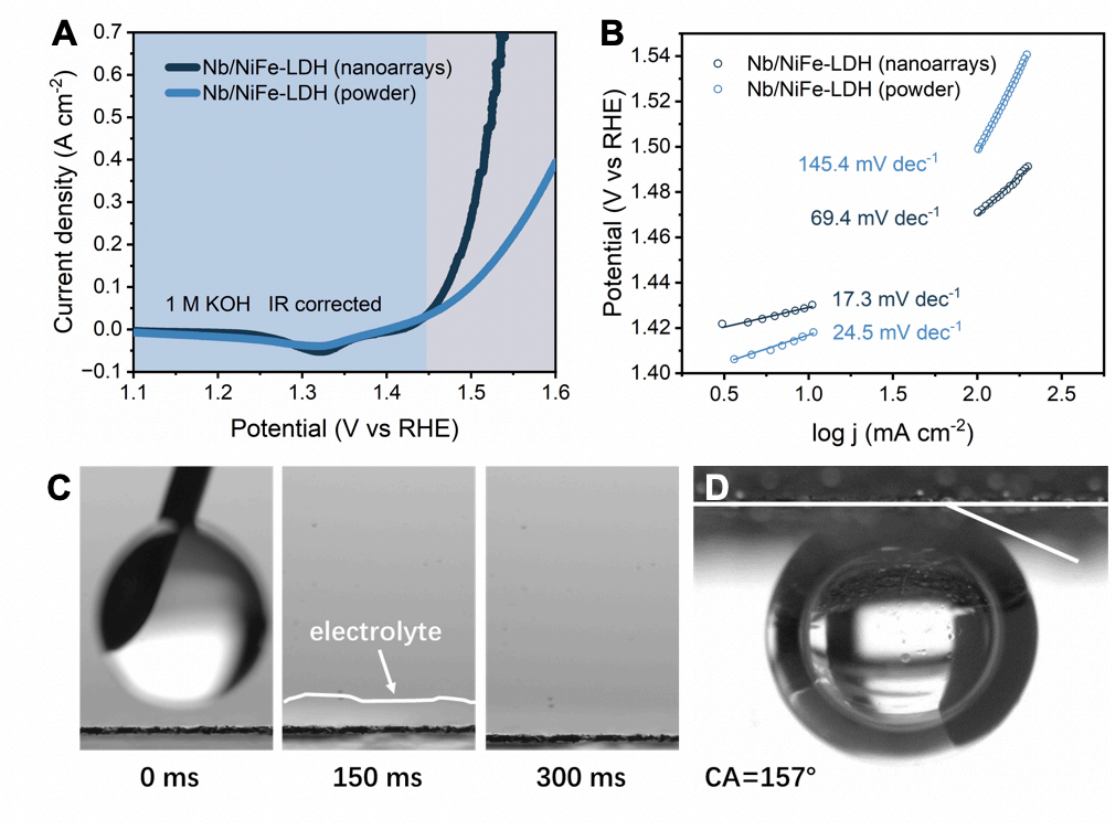

Figure 4. (A) Polarization curves of Nb/NiFe-LDH (nanoarrays) and Nb/NiFe-LDH (powder). (B) Tafel plots of Nb/NiFe-LDH (nanoarrays) and Nb/NiFe-LDH (powder). (C) Contact angle of Nb/NiFe-LDH (nanoarrays) with electrolyte. **d** (D) Contact angle of Nb/NiFe-LDH (nanoarrays) with bubble.

4. Conclusions

First, we enhanced the material's intrinsic catalytic activity. By doping the Nb^{5+} element, we increased the valence number of Ni and Fe, which helps form $Ni^{3+/4+}$ active sites. At the same time, a higher concentration of O-defect helps expose the active sites sufficiently, further improving the catalyst's intrinsic activity.

Second, we improved the performance of the catalytic media. The catalyst material we produced has a nanoarray structure that possesses superwettability and transfers the liquid reactants to the active sites at a high speed. In addition, it helps the gas product to break away quickly from the active sites. Hence, our Nb/NiFe LDH manifests a high current increase rate.

To conclude, by doping Nb into NiFe material that is grown on a self-supportive nanoarray base, we achieved a catalyst for the anode of water hydrolysis that has an outstanding electrocatalytic activity with good performance in both intrinsic activity and transfer media. Our material provides the design and manufacture of the OER catalyst with new inspiration and has the potential to be used in real water electrolysis in the future. Thus, our study result may contribute to the development of the hydrogen energy industry.

5. References

[1]. International Renewable Energy Agency (IRENA). (2022, July). China's route to carbon neutrality: Perspectives and the role of renewables. Retrieved from https://www.irena.org/publications/2022/Jul/Chinas-Route-to-Carbon-Neutrality

[2]. Hague, O. (2021, April 14). What are the 3 main types of hydrogen? Retrieved from https://www.brunel.net/en/blog/renewable-energy/3-main-types-of-hydrogen

[3]. Okamoto, Y. (2023, August 19). Chinese manufacturers dominate wind power, taking 60% of the global market. Retrieved from https://asia.nikkei.com/Business/Energy/Chinese-manufacturers-dominate-wind-power-taking-60-of-global-market

[4]. D. Zhou, P. Li, X. Lin, A. McKinley, Y. Kuang, W. Liu, W. Lin, X. Sun and X. Duan, Chem. Soc. Rev., 2021, 50, 8790.

[5]. Y. Liu, H. Wang, D. Lin, C. Liu, P.-C. Hsu, W. Liu, W. Chen and Y. Cui. Energy Environ. Sci., 2015, 8, 1719e24.

[6]. Y. Zhao, P. Zhang, J. Liang, X. Xia, L. Ren, L. Song, W. Liu and X. Sun. Advanced Materials. 2022, 34(37), 2204320.

[7]. W. Xu, Z. Lu, X. Sun, L. Jiang and X. Duan. Acc. Chem. Res. 2018, 51, 7, 1590–1598.

6. Acknowledgment

Thanks for permitting me to join and become a member of Beijing Youth's Top-notch Program.

Thanks for the opportunity offered by Beijing Youth Top-notch Program to get in contact with Prof. Sun Xiaoming and Beijing University of Chemical Technology.

Thanks for the opportunity offered by Prof. Sun to enter the university's lab and learn to do experiments. Thanks for lecturing us about the concepts in this field.

Thanks to the doctoral student, Liu Wei, in Prof. Sun's group for all the instruction and advice when I did the experiment and when I wrote this research article.

Thanks for all the support I have received so far.

Note that the topic was confirmed after I found and studied the field I was interested in and discussed it with Prof. Sun Xiaoming. Most of the experiment was done on my own and the data were collected on my own. The analysis of the data was partially helped by Liu Wei. The paper was completed on my own.